Spring 4-29-2020

A Study of the Antioxidant Versus Pro-Oxidant Nature of the Amyloid Beta Peptide and an Analysis of the Natural Products, Isorhamnetin and Narignenin, as Antioxidants

Kaylee Holmes

A STUDY OF THE ANTIOXIDANT VERSUS PRO-OXIDANT NATURE OF THE AMYLOID BETA PEPTIDE AND AN ANALYSIS OF THE NATURAL PRODUCTS, ISORHAMNETIN AND NARIGNENIN, AS ANTIOXIDANTS

by
Kaylee Grace Holmes

A thesis submitted to the faculty of The University of Mississippi in partial fulfillment of the requirements of the Sally McDonnell Barksdale Honors College.

Oxford May 2020

Approved by

Advisor: Professor Saumen Chakraborty

Reader: Professor Susan Pedigo

Reader: Professor James Cizdziel

Acknowledgements

The Sally McDonnell Barksdale Honors College
The University of Mississippi, Chemistry Department
The Chakraborty Lab
The Dass Lab
Dr. Chakraborty
Dr. Pedigo
Dr. Cizdziel
Suchitra Mitra

Abstract

KAYLEE GRACE HOLMES: A Study of the Antioxidant Versus Pro-oxidant Nature of the Amyloid Beta Peptide and an Analysis of the Natural Products, Isorhamnetin and Naringenin, as Antioxidants

(Under the direction of Dr. Saumen Chakraborty)

Alzheimer's disease is a neurodegenerative disorder with no cure. Due to the widespread effects of this disease, abundant research efforts have gone towards finding a cure. The amyloid beta (Aβ) peptide has been shown to be a potential cause of the disease due to destructive effects on tissues that it can have both by itself and through reactive oxygen species (ROS) generation. This study was performed in order to assess the structural properties of $A\beta_{42}$ monomers, fibrils and oligomers, to assess the antioxidant versus pro-oxidant behavior of the Aβ peptide, and to assess the antioxidant nature of the natural products isorhamnetin and naringenin. Several different ROS assays were performed in order to gain insight into the nature of $A\beta_{42}$, isorhamnetin, and naringenin. It was found that the oligomeric form of the peptide behaved solely as a pro-oxidant and generated much more ROS than the monomers and fibrils. The monomers and fibrils, however, showed antioxidant behavior as they decreased the amount of ROS generated by free copper under oxidative conditions. Isorhamnetin was far more successful at reducing ROS generation in all forms of the peptide than naringenin. After performing a copper titration, it was determined that two isorhamnetin molecules are able to bind one copper. These results indicate that $A\beta_{42}$ oligomers behave as pro-oxidants while $A\beta_{42}$ monomers and fibrils behave as antioxidants. The results also indicate that isorhamnetin is a better antioxidant than naringenin.

Table of Contents

List of Figures

List of Tables

Chapter 1: Introduction

1.1 Alzheimer's Disease

Worldwide, the leading cause of dementia is Alzheimer's Disease as 50-80% of all dementia cases are due to Alzheimer's.[1] According to the World Health Organization, there is approximately 18 million cases of Alzheimer's worldwide.[1] Its development has been found mostly in people over the age of 60, yet approximately 5% of all cases occur in people under the age of 60.[1] The Alzheimer's disease is a fatal neurodegenerative disease meaning there is loss of structure and function of the nerve cells that will eventually lead to death.[2] The type of nerve cells specifically affected in Alzheimer's are those of the cerebral cortex.[2] Due to the fact that there is no known cure for Alzheimer's Disease, it is not surprising that there is considerable research going towards finding a cure.[1]

The greatest risk factor in Alzheimer's Disease is increased age, and with humans progressively living longer, Alzheimer's Disease is becoming more and more prevalent.[1] In the next 20 years, the cases of the AD are expected to double, and by the year 2050, there is expected to be around 125 million cases of Alzheimer's disease.[1,3] With increasing AD cases expected to develop each year, there is also significant cost associated with the disease. According to the Alzheimer's Association and the National Institute on Aging, in the United States AD costs about $100 billion dollars annually (both direct and indirect costs included).[3] However, the invention of new treatments that could delay the onset of AD for even just five years would save the US and approximately $50 billion dollars

annually.[3] Taking into account the fatality of the disease as well as its estimated progression and financial burden, it is clear to see why finding a cure for the disease is a priority in the world of research.

1.2 The Role of Amyloid Beta in Alzheimer's Disease

In Alzheimer's Disease, there are two distinct pathologies that are found in the brain; extracellular plaque deposits of the amyloid-β peptide and the neurofibrillary tangles of the micro-tubule binding protein tau.[4,5] Although the tau protein does appear to be involved in the progression of AD, it is processed downstream of the amyloid-β peptide buildup.[6,9] Amyloid-β has two species: one consisting of 40 amino acids and the other consisting of 42 amino acids.[5] The $A\beta_{42}$ form is believed to be more neurotoxic.[8] Amyloid-β is generated by the cleavage of the transmembrane amyloid precursor protein (APP), where its N-terminus originates from the extracellular domain of APP and the C-terminus originating from the transmembrane region of APP.[5] When mutation occurs in APP, there is either an increased production of amyloid-β or an increased proportion of the amyloid-β-42 residue.[5] Many of the mutations in APP have little effect on its functionality but instead cause the tendency of amyloid-β to form fibrils.[7] Hereditary early onset forms of AD are linked to mutations within the amyloid-β precursor protein (AβPP), although these cases make up only about 1% of the total cases of AD.[1,4] APP undergoes substantial post-translational processing which can be in form of glycosylation, phosphorylation, and many other forms including various types of proteolytic processing to generate peptide fragments.[53] It is most commonly cleaved by proteases in the secretase family including alpha, beta, and gamma secretases. The alpha and beta secretases work to remove almost the entire extracellular

domain in order to release membrane-anchored carboxy-terminal fragments while the gamma secretases cleave within the membrane spanning domain.[54,55] The cleavage of beta secretases followed by the cleavage of gamma secretases leads to the generation of the amyloid peptide.[55] The cleavage of APP to form the amyloid-beta peptide is shown below in ***Figure 1***.

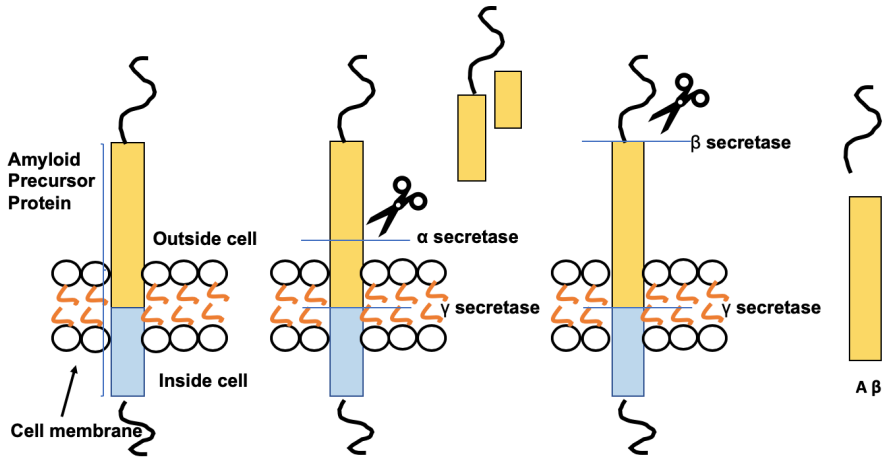

Figure 1. This figure illustrates the cleavage of APP to form the Aβ peptide. Here, the α, β, and γ secretases work to cleave APP from the membrane as well as to further cleave it into the Aβ peptide. The Aβ peptide is represented by the yellow rectangle and the blue rectangle as well as the black line represent the cleaved portions of APP. This process occurs during post-translational processing of APP.

In searching for the causative agent of AD, Hardy and colleagues published the amyloid cascade theory in which they proposed that the deposition of the amyloid-β peptide was the causative agent of AD.[9,10] With this hypothesis they also proposed that the neurofibrillary tangles of the tau protein, cell death, vascular destruction, and dementia followed as direct effects of the deposition of the amyloid-β peptide.[10] A study was also done in which mice were given the human gene for increased levels of $A\beta_{42}$ and it was found that they exhibited molecular, cellular and behavioral phenotypes similar to those found in AD.[11] However, there remain many substantial controversies with this theory. The most recurring controversy is the fact that amyloid-β deposits have been found in the

brains of humans who did not report or have symptoms of mental derange.[6] This controversy has been disputed by the fact that the deposits found in many of these subjects are of the diffuse type, meaning they do not have fibrillar amyloid, neuritic dystrophy or cytotoxiciticty.[6] Controversy has also been disputed by the fact that the soluble amyloid-β oligomers have not been quantified, and yet the peptide in the soluble oligomeric form is what is associated with the progression of AD.[6] Also, the subjects who were said to not have had signs of dementia (yet still had amyloid plaques), were not studied thoroughly enough to be confident whether or not they showed any signs of cognitive impairment.[6] In fact, it has been observed in seemingly normal subjects with amyloid deposits through amyloid-β imaging by positron emission tomography (PET), that there are often some cognitive deficiencies in such subjects.[6] Lastly, most chronic diseases show significant amounts of pathology prior to the diseases earliest symptoms.[6] With this being true, amyloid-β deposits in the brain cannot be dismissed for being linked to a cascade of neurodegeneration characteristic of AD.

Amyloid-β is a metalloprotein with several metal coordination residues and a hydrophobic core. These attributes along with its sequence are depicted below in ***Figure 2***. Amyloid-β peptide consists in three different structural forms: the monomeric form, the fibrillar form and the oligomeric form. Though the oligomeric form is thought to be the most toxic form, it is hard to fully distinguish due to its heterogeneous and metastable characteristics.[10] Originally, amyloid-β was thought to only be toxic in its fibrillar form, but when fibril formation was inhibited, neurotoxin formation still occurred.[11] The neurotoxin that was found was composed of small diffusible amyloid-β oligomers.[11] Because there are other molecules that appear in increased levels in AD affected brains,

there is a hypothesis that these molecules act as a chaperone to allow Aβ to self-associate, causing diffusible oligomers to form which are more harmful than even the fibrillary form of the amyloid peptide.[11] It was found that small amounts of a senile plaque protein slowly produced neurotoxin deposits in the central nervous system (CNS). These deposits were made of amyloid-β oligomers which were small, soluble, extremely diffusible, and toxic even in dilute nanomolar concentrations to mature CNS neurons.[11] This evidence is remarkable since one of the initial oppositions to amyloid-β being the causative agent for AD was the fact that it took tremendous amounts of the fibrillary form (initially believed to be the most toxic form) to kill neuronal cells.[12] Since the discovery that Aβ oligomers were indeed the most toxic form of the Aβ peptide, extreme efforts have been made in order to try and better understand the complex oligomeric form of Aβ on molecular and cellular levels.

DAEFRHDSGYEVHHQKLVFFAEDVGSNKGAIIGLMVGGVVIA

Figure 2. This figure shows the sequence for the $A\beta_{42}$ peptide. The amino acids highlighted in red indicate the metal coordinated residues and the amino acids highlighted in blue indicate the hydrophobic core of the peptide.

1.3 Amyloid Beta Oligomers: their pathway and toxicity

The amyloid peptide is intrinsically disordered meaning it does not have stable secondary or tertiary structures.[10] It can, however, still become folded or partially folded in particular conditions.[13] These conditions include conformational variations, pH, temperature, concentration of peptide and other external factors.[10,13] Due to the fact that the oligomeric form of amyloid-β is composed of a heterogenous mixture of intermediates

derived from several different pathways, the characterization of the oligomeric form has been extremely difficult and complex.[10] In addition, the longer Aβ residue ($A\beta_{42}$) introduces even greater variability (than the other major residue, $A\beta_{40}$) in its monomeric and fibrillary forms.[15] Atomic Force Microscope (AFM) images showing the different morphological features between Aβ fibrils and oligomers are shown below in ***Figure 3***.

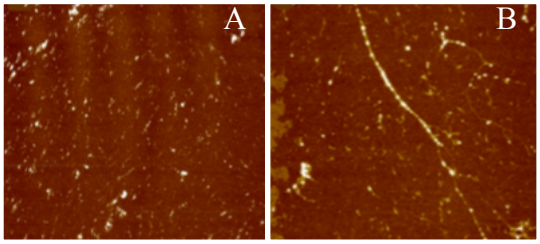

Figure 3. This figure shows AFM images taken of the A) oligomeric and B) fibrillar forms of the Aβ peptide.

Source: Mitra, Suchitra, Pallavi Prasad, and Saumen Chakraborty. "A Unified View of Assessing the Pro-oxidant versus Antioxidant Nature of Amyloid Beta Conformers." ChemBioChem 19.22 (2018): 2360-2371.

Before Aβ can self-aggregate at all, it first must be cleaved from APP via β- and γ-secretases. When Aβ monomers become partially folded, they tend to interact with one another.[13,15] This interaction allows their self-recognition sites to come in contact with each other and this promotes the beginning of self-aggregation.[13,15] This process is actually spontaneous because the interactions between these partially folded monomers are strong enough to overcome the original desire for disorder in the system. [10,13] Next, oligomeric species begin to form. Initially, small, toxic oligomers develop and begin to generate a nucleus.[10] The diverse, three-dimensional, Aβ species found in the nucleation process are referred to as on-pathway oligomers. These oligomers are later converted into larger aggregates or fibrillary Aβ units.[13,15] However, deviation from this pathway can occur, and the creation of this deviant species of oligomers are referred to as off-pathway oligomers. This deviation has been demonstrated by using polyphenol (-)-epigallocatechin gallate

(EGCG) in which EGCG was used to redirect the amyloid pathway and thus eliminate the possibility that amyloid fibrils would form.[16] Off-pathway oligomers are non-toxic and are stable final products unlike on-pathway oligomers which are an intermediary species for fibril formation during elongation.[16] This multistep process is shown below in ***Figure 4***.

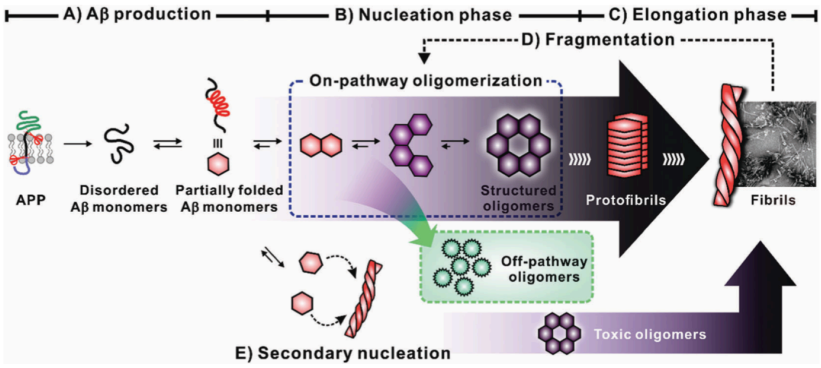

Figure 4. This figure illustrates Aβ production and aggregation. (A) Aβ production occurs due to the cleavage of APP by β- and γ-secretases. Natively the Aβ peptide is unfolded, but due to both environmental and genetic factors, they can become partially folded. (B) During on-pathway oligomerization, Aβ forms structured, transient oligomers which are suspected to be toxic. Off- pathway oligomers also form and are stabilized without further fibril growth. (C) Structured oligomers are metastable intermediates that further transform into protofibrils or fibrils. (D and E) Some fibrils can fragment and reassemble into structured oligomers (fragmentation). In addition, structured oligomers can be generated through interactions between monomers and fibrils (secondary nucleation).[10]

Source: Lee, Shin Jung C., et al. "Towards an understanding of amyloid-β oligomers: characterization, toxicity mechanisms, and inhibitors." Chemical Society Reviews 46.2 (2017): 310-323.

When Aβ monomers interact and aggregation occurs, as described previously, the process is called primary nucleation. However, Aβ monomers can instead interact with Aβ fibrils created downstream; this process is referred to as secondary nucleation.[17] The nucleation phase is the rate-determining step during amyloid fibrillation, with secondary nucleation being significantly faster than primary nucleation. When enough fibrils have formed to consistently interact with Aβ monomers, secondary nucleation becomes the dominant pathway for amyloid fibrillization.[17] In secondary nucleation, monomer-fibril interactions may cause the process of oligomer formation to be catalyzed.[17] Fibrils formed

through either pathway can dissociate into oligomers under certain stimulus such as force.[17] This is referred to as fibril fragmentation.[10] A study performed in 2013, suggested there is a positive feedback loop involving secondary nucleation and fibril fragmentation.[17] In the study, as the oligomeric reservoir grew greater (via fibril fragmentation), secondary nucleation was promoted, thereby further increasing the oligomeric reservoir at a faster and faster rate.[17] Therefore, oligomer formation can be produced through primary nucleation, secondary nucleation, and fibril fragmentation, and thus the oligomeric reservoir is continually increasing which means the toxicity levels also rapidly increase. This rapid rise in toxicity expedites the neurodegeneration in AD, and thus causes increased concern to learn how these oligomeric species can be suppressed.

Because it becoming more and more obvious that soluble, diffusible Aβ oligomers exhibit neurotoxicity in AD, the mechanisms by which they become toxic has become widely studied. There are three major mechanisms in which Aβ induces toxicity: interaction with membranes and synaptic receptors, intracellular system influence, and cell-to-cell transmission.[10] Extracellular amyloid-β oligomers can affect the cellular membrane in various ways. They can bind the membrane and in doing so cause damaging changes to the membrane. They can bind to signal transducing membrane receptors, thus either causing the cell to endocytose them, or generate damage due to abnormal signaling. They can cause the flow of substances into and out of the cell to be disrupted by penetrating the cell with circular structures that they form. *In vivo* and *in vitro* studies have shown that there is an interaction between Aβ oligomers and lipid rafts (membrane domains consisting of cholesterol, GM1-ganglioside sphingolipids, and synaptic receptors.)[18] In a study performed on Tg2576 transgenic mice, it was found that although the lipid rafts only make

up a small portion of total brain volume, they do contain 27% of $A\beta_{42}$ that is found in the brain and 24% of $A\beta_{40}$ that is found in the brain.[18] Because lipid rafts are involved in signal transduction, the accumulation of Aβ oligomers on lipid rafts could hinder signal transduction causing memory deficits.[10] This theory was supported by the Tg2576 transgenic mice study where the accumulation of Aβ on lipid rafts in 6 month on mice caused memory decline.[18] Other studies suggest that when Aβ interacts with membrane receptors, that synapse loss is initiated which is believed to be the link between neurodegeneration and cognitive impairment.[19] This interaction also promotes the endocytosis of oligomers, thus triggering further damage to the intracellular systems. [20] As previously mentioned, Aβ can also be generated and accumulated within the cell. This accumulation can cause many processes within the cell to have problems. Accumulation could cause stress to the endoplasmic reticulum (ER), calcium ion imbalance, mitochondrial damage, altered proteolysis, and ultimately these damages can cause cell death.[21] The final mechanism in which Aβ oligomers become toxic is through cell-to-cell transmission. The mechanism by which Aβ oligomers spread is very similar to the way that prion diseases spread.[14] A recent study was conducted in which autopsies of patients who had received cadaver-derived growth hormone, showed both the prion disease Creutzfeldt–Jakob disease (CJD), and amyloid-β plaque deposits. These patients had no genetic mutations linked with hereditary AD. The question arose as to whether or not Aβ pathology could be transmitted in humans similar to the way prion diseases are by way of seeding.[14,22] In a study performed on transgenic mice, concentrations of brain samples from AD patients were injected into the hippocampal formation or neocortex of the mice.[22] After a few days of incubation, there was no detectable trace of Aβ. However, after 3 to 5 months

post injection, Aβ deposits appeared and increased drastically the longer they were allowed to incubate.[22] The degree to which Aβ-seeding appeared in the mice was directly proportional to the concentrations of the brain samples that were injected into the mice.[22] The mice that had received brain extracts from non-AD infected brains showed no significant amounts of Aβ deposits.[22] The seeding mechanism that is believed to occur here is through a system of donor and acceptor neurons. The donor already contains the Aβ and the acceptor receives Aβ from the donor.[10,22] In a study performed by Nath and colleagues, Aβ was fluorescently labeled and was seen to be transferred from donor to acceptor cells. $A\beta_{42}$ showed the highest transmission rate out of the various isoforms of Aβ.[22] This cell-to-cell transmission produced large lysosomal vesicles that had the potential to dysregulate both the donor and acceptor cells. This is one pathway in which Aβ is believed to spread within the brain of AD patients.[14,22] However, more studies need to be performed to truly gain a complete view of Aβ transmission.

1.4 The Role of Metals and Reactive Oxygen Species in Alzheimer's Disease

The neurodegeneration that takes place in AD is also greatly impacted by the fact that Aβ is a metalloprotein, meaning that Aβ is metal-binding.[8] Metals are necessary for enzymatic function and often work to catalyze reactions, provide structural stability, and they play an important role in cellular signaling.[24] Therefore having a healthy balance of metals like iron, zinc, and copper, is an essential part of a healthy system.[24] However, in diseased brains, these concentrations become much higher than what is considered healthy.[8] Metal dyshomeostasis and abnormalities in the way metals are metabolized are thought to be directly involved with neurodegeneration in AD.[25] The amount of copper that

is deposited in the brain increases with age, but in AD patients this amount increases to concentrations as high as ~0.4 mM in the cerebral amyloid deposits.[8,23] In healthy cells, proteins tightly regulate copper, and no free copper is available because of this.[8] However, in diseased cells copper becomes unregulated, and hypermetalation occurs in copper proteins and Aβ peptides.[8] In Aβ, Cu^{2+} is believed to bind to His6, His13/His14, the terminal amine, an O atom (probably a part of the Ala2 backbone) and O-Asp1.[8,25] Under aerobic conditions and in the presence of biological reductants (such as ascorbic acid which is found at 0.2–10 mM concentrations in the brain), Cu^{2+} is reduced to Cu^{+}.[8] By way of the Fenton–Haber–Weiss reaction (shown in ***Scheme 1***), this reduction in copper gives rise to reactive oxygen species (ROS), which include O_2^{-}, H_2O_2 and $OH^{\bullet}$. Although copper bound Aβ is not the only source for copper reduction, it is the major source and thus accounts for the majority of ROS production.[8,23] This increase in free radical production leads way to an imbalance between the radicals and antioxidants in the body and thus causes oxidative stress.[26] The proposed structure for the copper-Aβ complex is shown in ***Scheme 1***.[27] Copper redox cycling is proposed to occur via a preorganized electron transfer (POET) mechanism.[28] This mechanism preorganizes the distances and angles within the Aβ-Cu coordination sphere so that it minimally rearranges upon electron transfer thus lowering the reorganization energy by 0.3 eV.[28] The POET mechanism leads to greater efficiency in redox cycling. The ROS created thorough this cycling oxidize cellular DNA, RNA, proteins and lipids, and therefore damage cellular function.[30] Lipid peroxidation occurs when ROS steal electrons from lipids, and this peroxidation produces 4-hydroxynonenal (HNE) which causes cellular damage specifically with cellular signaling.[8,29]

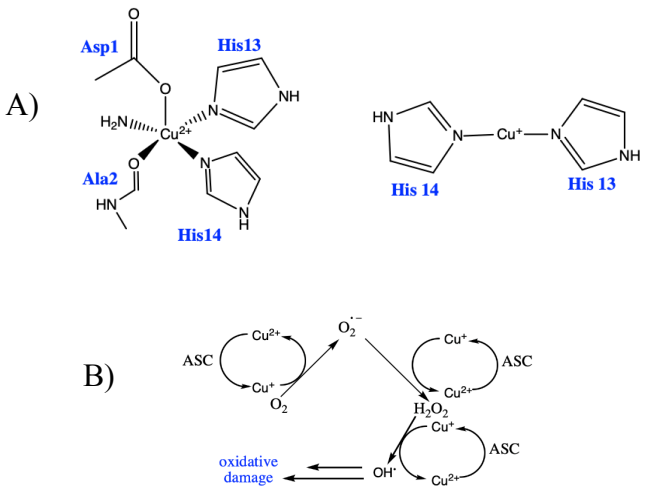

Scheme 1. (A) Proposed Cu^{2+}/Cu^{+} coordination of Aβ; (B) ROS generation by the Fenton-Haber-Weiss reaction.

Many studies have been performed to try and better understand Cu-catalyzed ROS production. It is still unclear whether Aβ plays an antioxidant role[31], a pro-oxidant role[32], or if it can be both an antioxidant and pro-oxidant within Cu-catalyzed ROS production.[33] The reasoning behind the antioxidant role of Aβ is due to the fact that in solution, the level of free radicals generated by Aβ is lower than the amount of free Cu^{2+}.[8] The reasoning behind the pro-oxidant role of Aβ is the fact that the Aβ-Cu complex generated more free radicals than other copper binding peptides.[8] Recent studies have shown that both the monomeric and fibrillar forms of Aβ can act as radical scavengers decreasing the amount of free radicals in vitro.[34] It has also been shown that $Aβ_{40}$ fibrils cause redox silencing, further deceasing the amount of free radicals.[35] Though information about the roles of the monomeric and fibrillar forms of Aβ has been studied and better understood, not much is understood about the role of the oligomeric form. Because the oligomeric form is considered the most neurotoxic form, it is important to further understand what role the oligomeric form plays in Cu-catalyzed ROS production.

1.5 The Role of Natural Products in Alzheimer's Disease Research

Many studies have suggested that there are dietary factors involved with the occurrence of AD, and in response, much research effort has gone towards understanding the influence that natural products have on Aβ toxicity. Specifically natural products with antioxidant properties and the ability to modulate small molecules are being researched as possible targets for AD.[36] These natural products can chelate metals and regulate metal homeostasis, alleviate oxidative stress, interact with Aβ both covalently and noncovalently, and redirect the Aβ aggregation pathway thus lowering the toxicity of potential aggregates.[37]

Flavonoids are a family of natural substances containing phenolic structures which are commonly found in fruits, vegetables, grains, bark, roots, stems, flowers, tea and wine.[44] Flavonoids are known for their health benefits specifically in regards to their anti-oxidative, anti-inflammatory, anti-mutagenic and anti-carcinogenic properties as well as their ability to regulate cellular enzymatic function.[44] In plants, flavonoids play a role in growth and defense against the formation of plaques which has made them very interesting in regards to AD research.[44] Flavonoids also have been shown to chelate iron and copper ions and therefore have been studied in regards to their potential relationship with metal-overload diseases as well as in situations regarding oxidative stress.[45] In a study performed by Holland and colleagues, it was concluded that higher dietary intake of flavanols may correspond to a decreased risk of developing dementia or Alzheimer's Disease.[47]

In this experiment, the natural flavonoids isorhamnetin and naringenin were selected in order to evaluate their ability to inhibit Cu-$A\beta_{42}$-induced ROS generation and regulation of the morphology of the monomeric, oligomeric and fibrillar species of the peptide under oxidative stress. Isorhamnetin (structure shown below in ***Figure 5A***) is an O-methylated

flavanol. This flavonoid is commonly isolated from water dropwort (Oenanthe javanica, Umbelliferae).[46] Pears, olive oil, wine, tomato sauce, and Mexican tarragon are also sources of isorhamnetin.[47,48] It has been shown to have antioxidant, anti-inflammatory, and anti-proliferative effects.[46] Naringenin (structure shown in ***Figure 5B***) is a flavanone commonly found in a variation of fruits and herbs and it is the major flavanone found in grapefruit.[49,50] This flavanone exists in two forms: the aglycol form (naringenin) and the glycosidic form (naringin), with the aglycol form being the most bioavailable.[51] Naringenin has been shown to have antioxidant effects as it decreases oxidative stress in cells.[52]

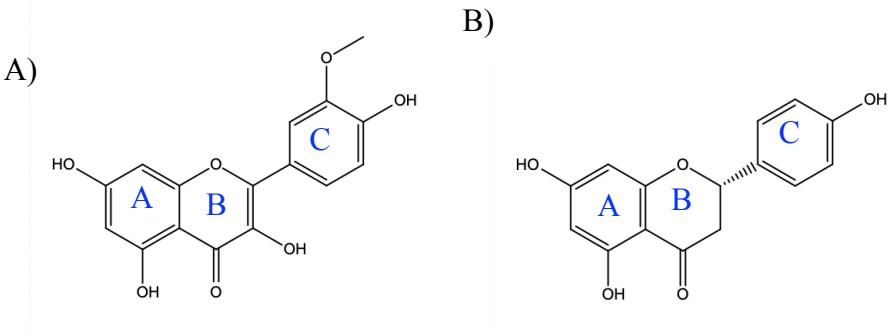

Figure 5. (A) Structure for isorhamnetin; (B) Structure for naringenin.

Studies have been performed on a similar flavonoid, kaempferol (shown below in ***Figure 6***), in which kaempferol decreased ROS production in all species of Aβ.[8] The study also demonstrated that two kaempferol molecules bind one Cu^{2+}.[8] The study accredited kaempferol's antioxidant abilities to three structural features: 1)its para-hydroxy group on its C-ring provides stability to aryloxy radicals through H bonding and takes part in electron dislocation, 2) its 2,3-double bond and 4-oxo group on its B-ring contribute to electron dislocation, 3) its 3- and 5-hydroxy groups that stabilize electron density from the C-ring.[8] We predicted that isorhamnetin and naringenin would behave in a similar way due to their similar structures. Isorhamnetin is structurally the same as kaempferol except for its added

methoxy group, and naringenin structurally the same as kaempferol except it is missing a hydroxy group on its B-ring.

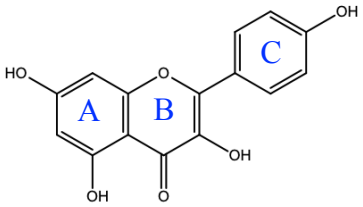

Figure 6. Structure for kaempferol.

Chapter 2: Methods

2.1 Synthesis and Purification of the Amyloid-β-42 Peptide

Synthesis

In this experiment, $A\beta_{42}$ (NH_3^+–$A\beta_{42}$-$CONH_2$) was synthesized using an automated microwave peptide synthesizer (Liberty Blue, CEM). This was done on a 0.1 millimolar scale using Rink Amide Pro-Tide Resin (CEM) with a poly(ethylene glycol) poly styrene backbone. In this study, the C-terminal amide was used because it tends to increased biological stability as well as an increased shelf-life. The coupling steps were performed at 90 ºC for 4 minutes. All amino acids (Advanced Chemtech) were weighed in concentrations of 0.2 M and dissolved in dimethylformamide (DMF; VWR). The activator base used was 1 M Oxyma (CEM) and the activator used was 0.5 M N,N'-diisopropylcarbodiimide (DIC; Advanced Chemtech) in DMF. The deprotection solution used was 20% piperidine (Advanced Chemtech) in DMF. Starting at His14, residues were double-coupled to guarantee that all amino acids were present in the synthesized peptide. Histidine residues were coupled at 50 ºC for 10 minutes to ensure that no racemization occurred.

Cleavage

In order to cleave the peptides from the resin and side-chain deprotection, the synthesized product was treated with 92.5% trifluoroacetic acid (TFA; Advanced Chemtech), 0.25% triisopropylsilane (TIS; Sigma–Aldrich), 0.25% ethane-1,2-dithol

(EDT; Sigma–Aldrich), and 0.25% water, in 10 mL volume. The product was treated for 2 hours at room temperature with continuous stirring. After cleavage, the crude peptides were filtered, and excess TFS was evaporated under a low flow of nitrogen gas. The crude peptides were then precipitated, washed with cold diethyl ether, dissolved in 10% acetic acid, and lyophilized. Then, the peptides were dissolved a second time in 10% acetic acid. After the peptides were dissolved in acetic acid, the peptides were ready for purification via High Performance Liquid Chromatography (HPLC).

High Performance Liquid Chromatography

Using a C_{18}-semiprep column (1260 Infinity II HPLC system, Agilent), the peptide was purified. The column compartment was kept at 75 ºC. A linear gradient from Solvent A (0.1% TFA in H_2O) to Solvent B (90% acetonitrile, 10% H_2O, 0.1% TFA) was used. Next, the peptide was injected at 1 $mL \cdot min^{-1}$ and eluted with 90% A and 10 % B for 5 minutes followed by a linear gradient to 70% B over 25 minutes at a flow rate of 4 $mL \cdot min^{-1}$. The peptide was eluted at about 50-60% Solvent B. The elution of the peptide was monitored via a chromatogram at 214 and 280 nm. The purified peptide was then lyophilized and stored in its monomeric form.

2.2 Preparation of Peptide Stocks

The purified and lyophilized peptide (1mM) was dissolved in 1,1,1,3,3,3-hexafluoropropan-2-ol (HFIP). These treated peptides were then placed in Eppendorf tubes (caps kept open) and left under the hood overnight. Next, the tubes were lyophilized in order to create films of completely unaggregated peptides. These peptides were kept at -80 ºC and used as needed.

In order to create a usable monomeric form of the peptide stocks, 100 μL of freshly made 10 mM NaOH (made from a freshly prepared 1 M NaOH stock) was placed into an Eppendorf tube containing the lyophilized and purified peptide (dissolved in HFIP). This tube was then vortexed for 30 seconds. After being vortexed, the tube was sonicated for 10 minutes at room temperature. Finally, the tube was centrifuged at 15000 g And room temperature for 3 minutes and immediately transferred to ice. The final concentrations of the monomeric peptides were then determined in cold water with an Agilent 8454 UV/Vis spectrophotometer by using Beer's Law (***Equation 1***) where ε_{280}=1490 $M^{-1}cm^{-1}$. Water with 10 mM NaOH was used as the blank.

2.3 Preparation of Amyloid-β-42 Fibrillar and Oligomeric Forms

Fibrillar Form

The fibrillar form of the peptide was prepared using premade monomeric peptides of known concentrations (as discussed in Section 2.3). Aβ monomers were mixed with phosphate buffered saline (PBS; pH 7.4) to achieve a fibril concentration of 100 μM. Once the PBS was added to the monomer, the tube was then incubated for 24 hours at 37 ºC. ***Figure 7B***, shown below, depicts this preparation.

Oligomeric Form

The oligomeric form of the peptide was also prepared using premade monomeric peptides of known concentrations (as discussed in Section 2.3). To achieve a final concentration of 25 μM, Aβ monomers were mixed with PBS (pH 7.4). Next, the mixture was centrifuged for 30 minutes at 15000 g and room temperature. Once the centrifugation was complete, the supernatant was taken from the tube and the pellet was disposed of. The

supernatant was then sonicated for 1 minute at room temperature. Once sonication was complete, the capped tube was allowed to sit at room temperature for 24 hours before being used experimentally. ***Figure 7A***, shown below, depicts this preparation.

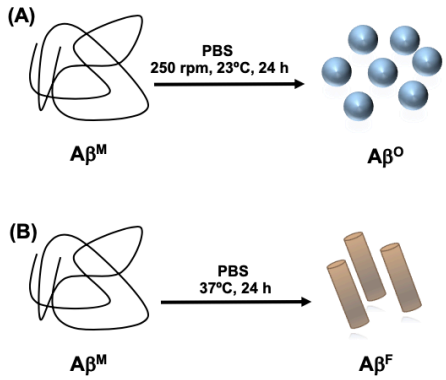

Figure 7. This figure depicts the methods of preparation of A) oligomers and B) fibrils used in this experiment.

2.4 Confirmation of Peptide Purity using MALDI-TOF MS

The identity and purity of the synthesized peptide stock was confirmed using MALDI-TOF MS (Bruker Voyager) with sinapinic acid (Sigma–Aldrich, 10 mg•mL^{-1} stock in ACN/H_2O (50:50) with 0.1% TFA) as the matrix. Using a ProteoMass calibration kit (Sigma-Aldrich) the instrument was externally calibrated. The sample, which contained a 1:1 ratio of peptide to matrix, was then loaded onto a MALDI plate and analyzed.

2.5 Preparation of Reagents

All buffer solutions were prepared in Milli-Q (Millipore) water and treated with Chelex 100 (Bio Rad) overnight to ensure that no trace metals remained in solution. The following day, the buffer was filtered using a buffer filter. The 1mM copper chloride stock solution (Alpha Aesar) was made in the presence of 40 mM glycine (Sigma-Aldrich) in order to prevent the precipitation of copper phosphate in the solution. This copper

chloride/glycine solution was the source of copper throughout the experiment. The ascorbic acid 10 mM stock solution (VWR) was prepared fresh daily in water. The 10 mM coumarin-3-carboxylic acid (3-CCA; Acros Organics) stock solution was prepared in phosphate buffer (PB; 20 mM; pH 9.0) at room temperature, and then was stored at -20 ºC. Prior to use, the 3-CCA was diluted with PB, and using either NaOH or H_3PO_4 the solution was adjusted to a pH of 7.4. The stock solutions of naringenin and isorhamnetin were dissolved in DMSO to a 7 mM concentration. The 10 mM Amplex Red stock solution was prepared in DMSO and stored at -20 ºC. The horseradish peroxidases (HRP) stock solutions were prepared at 10 Uml^{-1} in PB (pH 7.4).

2.6 Cu^{2+} Binding to Isorhamnetin

A Cu^{2+} binding titration of isorhamnetin was performed using an Agilent Cary 8454 UV-Vis spectrophotometer in a 1 cm path-length quartz cuvette. The solutions consisted of isorhamnetin (20 μM) in HEPES buffer (pH 7.4) with 1% DMSO added to the solution. For the blank scan, DMSO was substituted for the natural products in the solution. Cu^{2+} was added in 0.1 equivalent increments and was allowed to stir for 15 minutes before taking the measurement. When the UV-Vis spectra ceased to change, the Cu^{2+} had saturated the natural product and the titration was complete. Using the UV-Vis spectra, absorbance at an initial major peak λ versus the equivalents of copper added was plotted in order to determine how many equivalents of copper was necessary to saturate isorhamnetin. Though the same experiment was intended to be performed for naringenin, lab restrictions prohibited it from being conducted.

2.7 UV-Vis ASC Assay

UV-Vis spectroscopy is a widely used analytical method, most often utilized for its quantitative applications. It is commonly used to determine the concentration of analyte in solution by utilizing Beer's Law which is shown below in ***Equation 1***.

$$A=\varepsilon bc$$

Equation 1. This equation represents Beer's Law where A is equal to the absorbance, ε is equal to the molar extinction coefficient, b is equal to the path length and c is equal to the concentration of the analyte.[39]

A beam of UV and visible radiation is sent through a cuvette containing the sample. The sample solution then absorbs the light. How the sample absorbs the light is dependent on the concentration of the sample as well as the samples ability to absorb certain wavelengths of light. A detector, on the other side of the cuvette, is able to capture the amount of light that passes through the sample (this light was not absorbed by the sample).[40] The resulting data given by the UV-Vis spectrometer is the absorbance of light given at specific wavelengths. In order for UV-Vis spectroscopy to be used to analyze a sample, the sample must be known to absorb light within the UV or Visible region of the electromagnetic spectrum. In this region of the spectrum , electrons undergo electronic transitions. Common compounds that absorb in this region are transition metal ions, highly conjugated organic compounds, and biological macromolecules.[40]

In this study the kinetics of ascorbic acid (ASC) oxidation was monitored using an Agilent Cary 8454 UV-Vis spectrophotometer in a 1 cm path-length quartz cuvette. The decay of the ASC peak was monitored at 265 nm. The samples contained Aβ (5 μM), Cu^{2+} (4.5 μM), ASC (100 μM), naringenin (90 μM) and isorhamnetin (90μM). Chelated

phosphate buffer was added to the samples to reach a final volume of 320 μL. The composition of the samples that were used for analysis are shown below in ***Table 1***.

	Contents of the Sample
Sample 1	Aβ (monomer, oligomer, or fibril), ASC
Sample 2	Aβ (monomer, oligomer, or fibril), Cu^{2+}, ASC
Sample 3	Aβ (monomer, oligomer, or fibril), naringenin, ASC
Sample 4	Aβ (monomer, oligomer, or fibril), Cu^{2+}, naringenin, ASC
Sample 5	Aβ (monomer, oligomer, or fibril), isorhamnetin, ASC
Sample 6	Aβ (monomer, oligomer, or fibril), Cu^{2+}, isorhamnetin, ASC
Sample 7	Cu^{2+}, ASC

Table 1. This table shows the composition of each of the samples involved in the ASC assay. These samples were run individually for the monomeric, fibrillar, and oligomeric species of the Aβ peptide.

All components of the samples were mixed prior to the addition of ASC to ensure Cu^{2+} binding. Each sample (without ASC) was placed into the cuvette and a background reading was taken. The ASC was then added to the cuvette and mixed via pipette mixing. Immediately following the addition of ASC, the analysis was started. The UV-Vis spectrophotometer was set to take a reading once every 60 seconds for a total of 3300 seconds. Each experiment was performed at least three times with different preparations of each Aβ species (monomers, oligomers, and fibrils).

2.8 Fluorescence Hydroxyl Radical Assay

Fluorescence spectroscopy is a type of electromagnetic spectroscopy that analyzes the fluorescence given off by a sample. It uses a beam of light, usually ultraviolet, to excite the electrons in a molecule and the excitation causes them to emit light.[41] The molecule is first excited through the absorption of a photon, from its ground electronic state to a vibrational state in the molecules excited electronic state.[42] When the excited molecule collides with other molecules, it loses vibrational energy until it reaches the lowest vibrational state possible within that excited electronic state.[42] This process is shown in a Jablonski diagram.[42]

In this experiment, the Cu-Aβ species was probed to produce $OH^{\bullet}$ by the Fenton-Haber-Weiss Reaction using a colorimetric CCA-3 assay. The kinetics of the oxidation of 3-CCA to the fluorescent molecule, 7-hydroxycoumarin-3-carboxylic acid (7-OH-CCA) , by the hydroxyl radical, $OH^{\bullet}$, were monitored. This was done using a PTI fluorimeter with the $\lambda_{excitation}$ set at 395 nm and the $\lambda_{emission}$ set at 450 nm. These wavelengths are where the fluorescent molecule, 7-OH-CCA, can be detected. The samples contained Aβ peptides (10 μM), Cu^{2+} (9μM), 3-CCA (100 μM) and ASC (100 μM). Chelated phosphate buffer was added to the samples to reach a final volume of 320 μL. These assays were performed at a 2:1 Aβ/Cu^{2+} ratio. The natural products (isorhamnetin and naringenin) were not analyzed in this assay because they were dissolved in DMSO which can scavenge $OH^{\bullet}$ and thus alter results.[43] The composition of the samples that were used for analysis are shown below in ***Table 2***.

	Contents of the Sample

Sample 1	Aβ (monomer, oligomer, or fibril), CCA, ASC
Sample 2	Aβ (monomer, oligomer, or fibril), Cu^{2+}, CCA, ASC
Sample 3	Cu^{2+}, CCA, ASC

Table 2. This table shows the composition of each of the samples involved in the $OH^{\bullet}$ assay. These samples were run individually for the monomeric, fibrillar, and oligomeric species of the Aβ peptide.

All components of the samples were mixed prior to the addition of ASC. Each sample (without ASC) was placed into the cuvette and a background emission scan was taken. The ASC was then added to the cuvette and mixed via pipette mixing. Immediately following the addition of ASC, the analysis was begun. The fluorimeter was set to obtain one scan every 60 seconds for 3000 seconds. Each experiment was performed at least three times with different preparations of each Aβ species (monomers, oligomers, and fibrils).

2.9 UV-Vis H_2O_2 Assay

An Agilent Cary 8454 UV-Vis spectrophotometer in a 1 cm path-length quartz cuvette was used to monitor the Cu^{2+}-catalyzed H_2O_2 formation. In the presence of HRP, Amplex Red reacts with H_2O_2 to produce the chemical resorufin, and therefore resorufin was monitored as a direct measure of the relative amount of H_2O_2 produced.[8] Resorufin absorbs strongly at 572 nm.[8] The samples for the H_2O_2 assays with peptides consisted of Aβ (5 μM), Cu^{2+} (4.5 μM), Amplex Red (50 μM), HRP (0.1 UmL^{-1}), ASC (100 μM), naringenin (90 μM), isorhamnetin (90μM), and 1% DMSO which was added to the samples in order to ensure that the natural products remained soluble. Chelated phosphate buffer

was added to the samples to reach a final volume of 320 μL. The composition of the samples that were used for analysis are shown below in ***Table 3***.

	Contents of the Sample
Sample 1	Aβ (monomer, oligomer, or fibril), Amplex Red, HRP, DMSO, ASC
Sample 2	Aβ (monomer, oligomer, or fibril), Cu^{2+}, Amplex Red, HRP, DMSO, ASC
Sample 3	Aβ (monomer, oligomer, or fibril), naringenin, Amplex Red, HRP, DMSO, ASC
Sample 4	Aβ (monomer, oligomer, or fibril), Cu^{2+}, naringenin, Amplex Red, HRP, DMSO, ASC
Sample 5	Aβ (monomer, oligomer, or fibril), isorhamnetin, Amplex Red, HRP, DMSO, ASC
Sample 6	Aβ (monomer, oligomer, or fibril), Cu^{2+}, isorhamnetin, Amplex Red, HRP, DMSO, ASC
Sample 7	Cu^{2+}, Amplex Red, HRP, DMSO, ASC

Table 3. This table shows the composition of each of the samples involved in the H_2O_2 assay. These samples were run individually for the monomeric, fibrillar, and oligomeric species of the Aβ peptide.

All components of the samples were mixed prior to the addition of ASC to ensure Cu^{2+} binding. Each sample (without ASC) was placed into the cuvette and a background reading was taken. The ASC was then added to the cuvette and mixed via pipette mixing. Immediately following the addition of ASC, the analysis was begun. The production of H_2O_2 was monitored at 572 nm. The UV-Vis spectrophotometer was set to take a reading once every 60 seconds for a total of 3300 seconds. Each experiment was performed at least

three times with different preparations of each Aβ species (monomers, oligomers, and fibrils).

Chapter 3: Results and Discussion

3.1 Confirmation of Peptide Purity using MALDI-TOF MS

HPLC was performed in order to purify the peptide after synthesis. The HPLC chromatogram is shown below in ***Figure 8***.

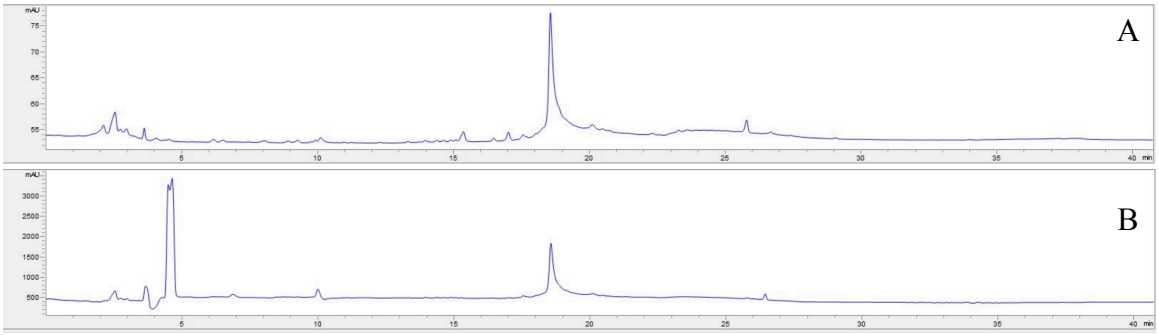

Figure 8. This figure shows the chromatogram that was generated by HPLC during purification. (A) This plot was monitored at 280 nm where tyrosine can be observed. Because $A\beta_{42}$ contains tyrosine, it can be monitored to indicate the presence of $A\beta_{42}$ during HPLC. The peak at approximately 18.5 minutes indicates the purified peptide. (B) This plot was monitored at 215 nm where the peptide bond can be observed. This peak also occurred at approximately 18.5 minutes and is therefore where the peptide was collected.

After HPLC purification was complete, MALDI-MS was used to verify that purity of the peptide. Using MALDI-MS, the spectrum shown in ***Figure 9*** was found for the purified Aβ peptide. A strong peak at 4513 m/z emerged which corresponds to the molecular weight of the $A\beta_{42}$ peptide which is 4514 Da.[38] This spectrum ensures that following HPLC, that the peptide was purified and ready to be used experimentally.

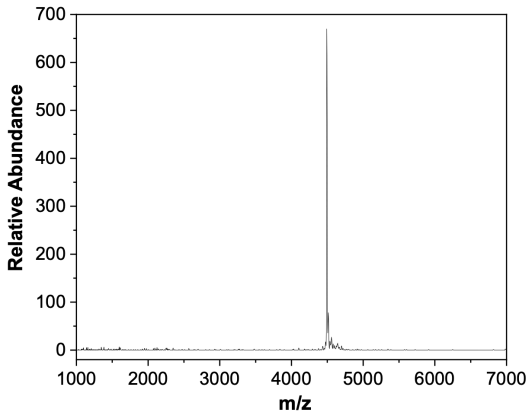

Figure 9. MALDI-MS of the purified Aβ peptide stock. The strong peak at 4513 m/z corresponds to the molecular weight of the Aβ peptide.

3.2 Cu^{2+} Binding to Isorhamnetin

The ability of isorhamnetin to chelate Cu^{2+} and scavenge ROS generated by Cu-Aβ species was monitored in this experiment. First, titration was used to monitor this. Gradual amounts of Cu^{2+} were added to the isorhamnetin solution and spectra changes were observed until saturation was reached and no further changes occurred. This spectra is shown below in ***Figure 10***. Two major peaks at 271 nm and 378 nm and one minor peak at 321 nm from isorhamnetin decayed and eventually two new major peaks at 252 nm and 319 nm formed as isorhamnetin became saturated with copper. This indicates that isorhamnetin successfully binds copper.

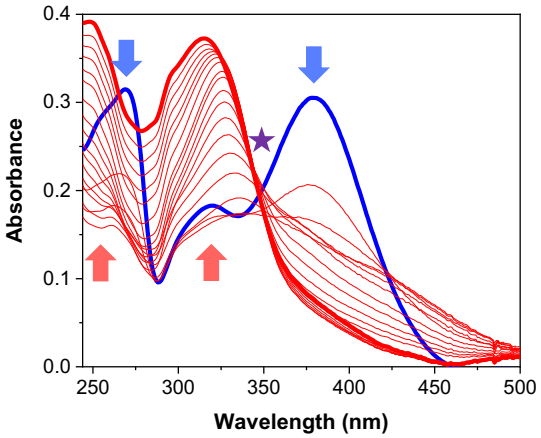

Figure 10. UV/Vis spectra of Cu^{2+} binding titration to a solution containing 10 µM isorhamnetin in 20 mM HEPES buffer (pH 7.4). The starting isorhamnetin spectrum is shown in blue. Subsequent spectra from Cu^{2+} binding are shown in less intense red, with the final Cu-isorhamnetin spectrum shown as thick red. The disappearance and emergence of major peaks are shown as blue and red arrows, respectively. The star is placed directly above the isosbestic point on the plot which indicates the wavelength at which the absorbance did not change throughout the course of the experiment.

By plotting the absorbance peak at 378 nm against the equivalents of Cu^{2+} added, it was found that 0.5 equivalents of copper binds to 1 equivalent of isorhamnetin (***Figure 11***). Unfortunately this titration was unable to be repeated due to laboratory restrictions caused by COVID-19. Ideally, there would be no decrease in slope after the saturation point at 0.5 equivalents.

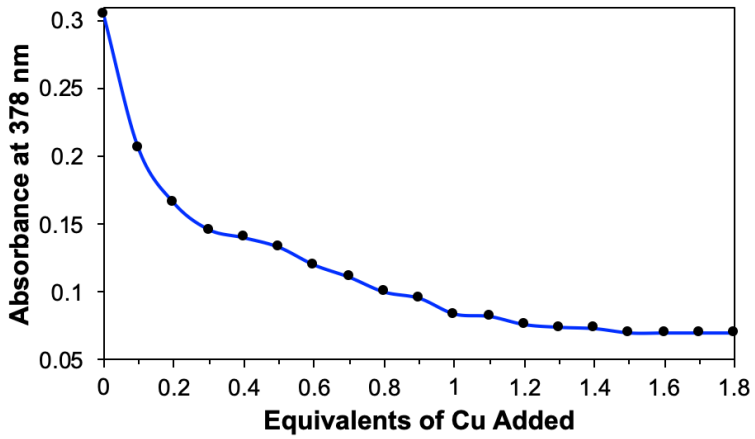

Figure 11. This figure shows absorbance at 378 nm (where a major peak decayed) versus the equivalents of copper added. The sample reaches complete saturation at approximately 0.5 equivalents of copper where the slope of the line ceases to decrease drastically. Therefore, 0.5 equivalents of copper is needed to bind one equivalent of isorhamnetin. In other words, 2 isorhamnetin molecules are needed to bind 1 copper.

Kaempferol, a compound with a similar structure to isorhamnetin is believed to bind 1 copper with 2 kaempferol molecules. This bond is formed between the two hydroxyl groups on ring B (shown in ***Figure 6***) on two different kaempferol molecules (four hydroxyl groups total) to one copper molecule. Because the saturation ratio is the same for isorhamnetin to copper, ***Figure 12*** proposes a potential way in which isorhamnetin binds copper.

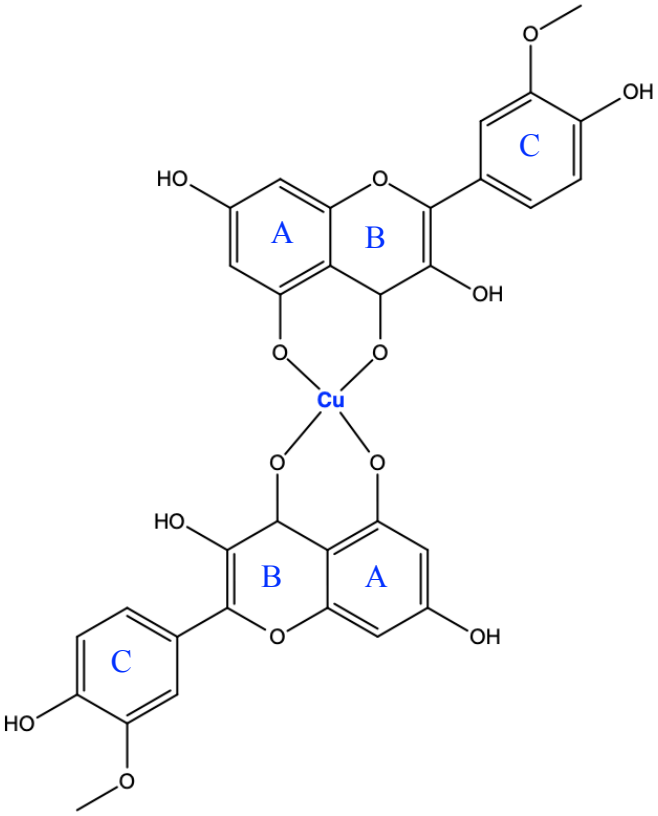

Figure 12. This figure proposes a way in which 2 equivalents of isorhamnetin could bind 1 equivalent of copper.

Though isorhamnetin seems like it may work equal to kaempferol as an antioxidant, isorhamnetin also has a potentially pro-oxidant feature. Due to the addition of a methoxy group on ring C (as compared to kaempferol), it is believed that this electron donating group may give electrons to Cu^{2+} causing Cu^{+} to be stabilized.

According to the Fenton-Haber-Weiss reaction (shown in ***Scheme 1B***), Cu^{+} leads to ROS generation and therefore this portion of isorhamnetin is believed to also exhibit pro-oxidant behavior.

Ideally, this titration would have also been performed for naringenin, but due to lab restrictions caused by COVID-19, this was not possible.

3.3 UV-Vis ASC Assay

In this experiment, ASC oxidation was used as a direct measure of the amount of ROS produced by different species of the Aβ peptide. This was performed using 10 μM peptide and 9 μM Cu^{2+} in the presence of tenfold excess of ASC. ASC oxidation was monitored over the course of 3000 seconds by the decay of an absorbance peak at 265 nm. The oligomeric form of Aβ ***(Figure 13B)*** consumed ASC the fastest compared to the monomeric form, fibrillar form, and free Cu. This indicates that the oligomeric form generates more ROS in a shorter amount of time.

To test the effect of isorhamnetin and naringenin on ASC oxidation, they were added with a tenfold excess with respect to Cu^{2+} to the different species of the Aβ peptide. Naringenin did not show much decrease in the generation of ROS production, instead it only slightly decreased the ROS production in the monomeric form of the peptide, but not in any of the other forms. Isorhamnetin moderately decreased the amount of ROS produced in all species of the Aβ peptide as shown by the royal blue line in ***Figure 13***. It reduced ROS production the most for the fibrillar form of the peptide as seen in ***Figure 13C***. Compared to a study performed by Chakraborty and colleagues using the natural product

kaempferol, the natural products isorhamnetin and naringenin are not as effective at reducing ROS production as kaempferol.[8]

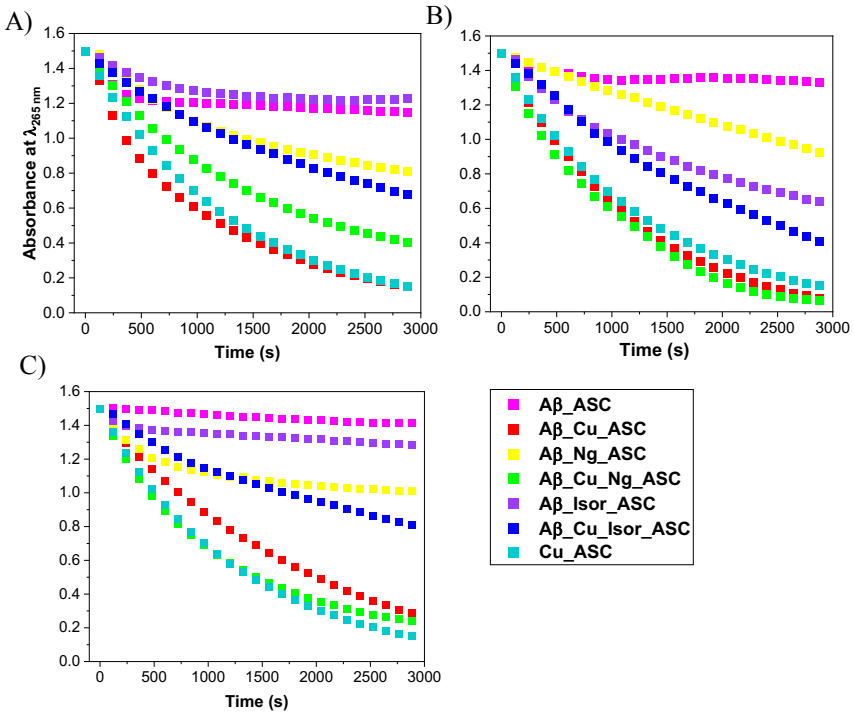

Figure 13. In this figure, as ASC is consumed, less absorbance is detected. Here, ASC consumption is used as a direct measure of ROS production. (A) Aβ monomer, (B) Aβ oligomer, (C) Aβ fibril.

3.4 Fluorescence Hydroxyl Radical Assay

Using a colorimetric 3-CCA assay, the ability of each Cu-Aβ species to produce $OH^{\bullet}$ by the Fenton-Haber-Weiss reaction was assessed. Consistent with the ASC oxidation and H_2O_2 experiments, the oligomeric form of the peptide showed the highest rate of $OH^{\bullet}$ production compared to the monomeric and fibrillar forms of the peptide. This can be seen in ***Figure 14***, where the red line in ***Figure 14B*** increases more than the red line in ***Figure 14A*** (monomer) and ***Figure 14C*** (fibril). In all cases the amount of $OH^{\bullet}$ produced by free Cu^{2+} (shown by the turquoise line in ***Figure 14***) was much greater than the amount produced by the Cu-Aβ complex. The lower amount of $OH^{\bullet}$ produced by the monomeric

and fibrillar forms of the peptide suggest that they effectively scavenge $OH^{\bullet}$, and thus hinder the production of the fluorescent molecule, 7-OH-CCA. Therefore, these forms of the peptide appear to behave as antioxidants against radicals. The increased production of $OH^{\bullet}$ in this study along with the increase in ROS production in both the ASC and H_2O_2 assays indicates that the oligomeric form acts as a pro-oxidant. The differences in $OH^{\bullet}$ production between each of the Aβ species indicates that there are inherent differences in the structure of their Cu binding complexes which changes the efficiency of electron transport and thus the amount of ROS produced also is affected.

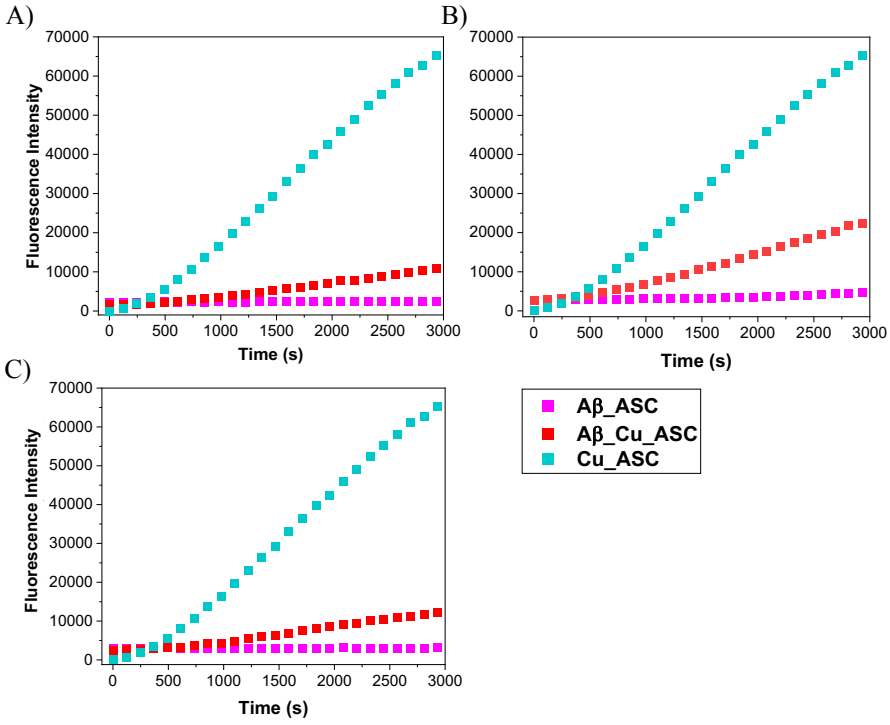

Figure 14. This figure shows the production of the fluorescent molecule 7-OH-CCA, thus indicating that $OH^{\bullet}$ radical was produced. The higher the intensity on the plot, the more $OH^{\bullet}$ was produced. (A) Aβ monomer, (B) Aβ oligomer, (C) Aβ fibril.

3.5 UV-Vis H_2O_2 Assay

The relative amounts and rates of H_2O_2 production by each Aβ species was monitored in this assay by the detection of resorufin at 572 nm. The data retrieved is shown below in ***Figure 15***. The oligomeric form of the peptide produced substantial amounts of H_2O_2 with the absorbance shown to reach about 1.2. The monomeric form of the peptide produced less than the oligomeric form of the peptide with its maximum absorbance shown to reach about 0.8. The fibrillar form of the peptide, generated far less H_2O_2 with its maximum absorbance only reaching half of what the oligomeric form did (about 0.6). The monomeric and oligomeric forms of the Cu-Aβ complex showed to produce more H_2O_2 than free Cu^{2+}. This was only substantial for the oligomeric form since about two times the amount of H_2O_2 was generated for the Cu-$A\beta^O$ complex than was generated for free Cu^{2+} in solution. This confirms the pro-oxidant role of the oligomeric form of the peptide. Though the Cu-$A\beta^M$ complex showed to generate more H_2O_2 than free Cu^{2+} it was not major at all, and thus does not imply a pro-oxidant role of the monomeric form, and does not negate the antioxidant properties shown in the ASC oxidation assay. The fibrillar form showed a substantial decrease in H_2O_2 production compared to that produced by free Cu^{2+} in solution, therefore confirming the antioxidant role of the fibrillar form demonstrated in the ASC oxidation assay.

Isorhamnetin showed a substantial decrease in the amount of H_2O_2 production in all forms of the peptide, with in all cases the amount of H_2O_2 produced being less than that of even just Aβ in solution (without Cu^{2+}). Naringenin, however, showed minimal decrease in H_2O_2 production. Overall, in both the ASC oxidation study and in the H_2O_2 study, isorhamnetin was much better at decreasing ROS production than naringenin.

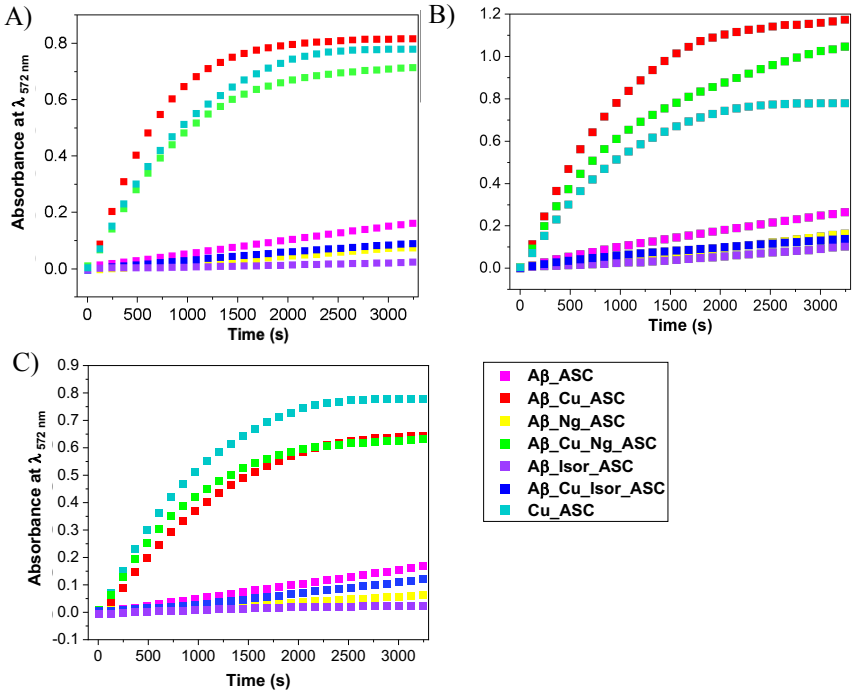

Figure 15. Top left: Monomer, Top Right: Oligomer, Bottom: Fibril

Chapter 4: Conclusion

This study was performed in order to assess the structural properties of $A\beta_{42}$ monomers, fibrils and oligomers, to assess the antioxidant versus pro-oxidant behavior of the Aβ peptide, and to assess the antioxidant nature of the natural products isorhamnetin and naringenin.

First, the synthesis and purification of $A\beta_{42}$ was performed, and then the purification of the peptide was evaluated using MALDI-MS. After retrieving the purified peptide, monomers, oligomers, and fibrils were all prepared. Several different assays were performed using all forms of the peptide as well as in some cases the natural products naringenin and isorhamnetin.

The first assay performed was an ASC assay performed on a UV-Vis spectrometer (***Figure 13***). It was found that the oligomeric form of the peptide generated more ROS in a shorter amount of time than the other forms, as it to be expected. It was also found that naringenin did not show a major decrease in the generation of ROS production. Isorhamnetin, on the other hand, did moderately decrease the amount of ROS produced in all species of the Aβ peptide, with the most decrease occurring in the fibrillar form.

The second assay performed was fluorescence hydroxyl radical assay. The purpose of this assay was to determine which form of the peptide behaved most as a pro-oxidant as well as to verify the antioxidant nature of the monomeric and fibrillar forms of the peptide. This experiment was successful as it can be seen in ***Figure 14*** that the

oligomeric form produced considerably more hydroxyl radical than the other two forms of the peptide.

The final assay that was performed was an H_2O_2 assay performed on a UV-Vis spectrometer. This assay monitored the relative amount of H_2O_2 produced upon the presence of ASC in the sample. This experiment showed similar results to the ASC assay. The oligomeric form of the peptide produced considerably more amounts of H_2O_2 than the other forms of the peptide. Isorhamnetin showed a major decrease in the amount of H_2O_2 production in all forms of the peptide, with in all cases the amount of H_2O_2 produced being less than that of even just Aβ in solution (without Cu^{2+}). Naringenin, however, showed minimal decrease in H_2O_2 production.

Overall it was found that isorhamnetin was drastically more effective in decreasing ROS species than naringenin. This was shown in both the ASC and H_2O_2 assays. In order to determine the binding capability of isorhamnetin to copper, a copper binding titration was performed with isorhamnetin and it was found that 1 equivalent of isorhamnetin binds 0.5 equivalents of copper. In other words, 2 isorhamnetin molecules were needed to bind one copper molecule. The proposed isorhamnetin-copper complex is shown in ***Figure 12***.

The results of this study indicate that $A\beta_{42}$ oligomers behave as pro-oxidants while $A\beta_{42}$ monomers and fibrils behave as antioxidants. The results also indicate that isorhamnetin is a better antioxidant than naringenin.

LIST OF REFRENCES:

1. Hamley, I. W. “The Amyloid Beta Peptide: A Chemist’s Perspective. Role in Alzheimer’s and Fibrillization.” *Chemical Reviews*, vol. 112, no. 10, 2012, pp. 5147–5192., doi:10.1021/cr3000994.
2. Przedborski, Serge, et al. “Series Introduction: Neurodegeneration: What Is It and Where Are We?” *Journal of Clinical Investigation*, vol. 111, no. 1, 2003, pp. 3–10., doi:10.1172/jci200317522.
3. Mount, Claire, and Christian Downton. “Alzheimer Disease: Progress or Profit?” *Nature Medicine*, vol. 12, no. 7, 2006, pp. 780–784., doi:10.1038/nm0706-780.
4. Murphy, M. Paul, and Harry LeVine III. "Alzheimer's disease and the amyloid-β peptide." *Journal of Alzheimer's disease*19.1 (2010): 311-323.
5. Goedert, Michel, and Maria Grazia Spillantini. "A century of Alzheimer's disease." *science* 314.5800 (2006): 777-781.
6. Selkoe, Dennis J. "Resolving controversies on the path to Alzheimer's therapeutics." *Nature medicine* 17.9 (2011): 1060.
7. Wisniewski, Thomas, et al. “Peptides Homologous to the Amyloid Protein of Alzheimer's Disease Containing a Glutamine for Glutamic Acid Substitution Have Accelerated Amyloid Fibril Formation.” *Biochemical and Biophysical Research Communications*, vol. 179, no. 3, 1991, pp. 1247–1254., doi:10.1016/0006-291x(91)91706-i.
8. Mitra, Suchitra, Pallavi Prasad, and Saumen Chakraborty. "A Unified View of Assessing the Pro-oxidant versus Antioxidant Nature of Amyloid Beta Conformers." *ChemBioChem* 19.22 (2018): 2360-2371.
9. Hardy, John. "Alzheimer's Disease: The Amyloid Cascade Hypothesis: An Update and Reappraisal." *Journal of Alzheimer's Disease : JAD*, vol. 9, no. 3 Suppl, 2006, pp. 151-153.
10. Lee, Shin Jung C., et al. "Towards an understanding of amyloid-β oligomers: characterization, toxicity mechanisms, and inhibitors." *Chemical Society Reviews* 46.2 (2017): 310-323.
11. Lambert, M P et al. “Diffusible, nonfibrillar ligands derived from Abeta1-42 are potent central nervous system neurotoxins.” *Proceedings of the National Academy of Sciences of the United States of America* vol. 95,11 (1998): 6448-53. doi:10.1073/pnas.95.11.6448
12. Seubert, Peter, et al. "Isolation and quantification of soluble Alzheimer's β-peptide from biological fluids." *Nature* 359.6393 (1992): 325-327.

13. Chiti, Fabrizio, and Christopher M. Dobson. "Protein Misfolding, Functional Amyloid, and Human Disease." *Annual Review of Biochemistry*, vol. 75, 2006, pp. 333.

14. Jaunmuktane, Zane, et al. "Evidence for Human Transmission of Amyloid-β Pathology and Cerebral Amyloid Angiopathy." *Nature*, vol. 525, no. 7568, 2015, pp. 247-250.

15. Miller, Yifat, Buyong Ma, and Ruth Nussinov. "Polymorphism in Alzheimer Aβ amyloid organization reflects conformational selection in a rugged energy landscape." *Chemical reviews*110.8 (2010): 4820-4838.

16. Ehrnhoefer, Dagmar E., et al. "EGCG Redirects Amyloidogenic Polypeptides into Unstructured, Off-Pathway Oligomers." *Nature Structural & Molecular Biology*, vol. 15, no. 6, 2008, pp. 558-566.

17. Samuel I. A. Cohen, et al. "Proliferation of Amyloid-β42 Aggregates Occurs through a Secondary Nucleation Mechanism." *Proceedings of the National Academy of Sciences of the United States of America*, vol. 110, no. 24, 2013, pp. 9758-9763.

18. Kawarabayashi, Takeshi, et al. "Dimeric amyloid β protein rapidly accumulates in lipid rafts followed by apolipoprotein E and phosphorylated tau accumulation in the Tg2576 mouse model of Alzheimer's disease." *Journal of Neuroscience* 24.15 (2004): 3801-3809.

19. Talantova, Maria, et al. "Aβ induces astrocytic glutamate release, extrasynaptic NMDA receptor activation, and synaptic loss." *Proceedings of the National Academy of Sciences*110.27 (2013): E2518-E2527.

20. Lai, Aaron Y., and JoAnne McLaurin. "Mechanisms of amyloid-Beta Peptide uptake by neurons: the role of lipid rafts and lipid raft-associated proteins." *International journal of Alzheimer's disease* 2011 (2011).

21. Umeda, Tomohiro, et al. "Intraneuronal amyloid β oligomers cause cell death via endoplasmic reticulum stress, endosomal/lysosomal leakage, and mitochondrial dysfunction in vivo." *Journal of neuroscience research* 89.7 (2011): 1031-1042.

22. Walker, Lary C., Juliane Schelle, and Mathias Jucker. "The prion-like properties of amyloid-β assemblies: implications for Alzheimer's disease." *Cold Spring Harbor perspectives in medicine* 6.7 (2016): a024398.

23. Bush, Ashley I. "The Metallobiology of Alzheimer's Disease." *Trends in Neurosciences*, vol. 26, no. 4, 2003, pp. 207-214.

24. Roberts, Blaine R., et al. "The Role of Metallobiology and Amyloid-β Peptides in Alzheimer's Disease." *Journal of Neurochemistry*, vol. 120 Suppl 1, 2012, pp. 149.

25. Faller, Peter, and Christelle Hureau. "Bioinorganic chemistry of copper and zinc ions coordinated to amyloid-β peptide." *Dalton Transactions* 7 (2009): 1080-1094.

26. Greenough, Mark A., James Camakaris, and Ashley I. Bush. "Metal dyshomeostasis and oxidative stress in Alzheimer's disease." *Neurochemistry international* 62.5 (2013): 540-555.
27. Shearer, Jason, and Veronika A. Szalai. "The Amyloid-β Peptide of Alzheimer's Disease Binds CuI in a Linear Bis-His Coordination Environment: Insight into a Possible Neuroprotective Mechanism for the Amyloid-β Peptide." *Journal of the American Chemical Society*, vol. 130, no. 52, 2008, pp. 17826-17835.
28. Balland, Véronique, Christelle Hureau, and Jean-Michel Savéant. "Electrochemical and homogeneous electron transfers to the Alzheimer amyloid-β copper complex follow a preorganization mechanism." *Proceedings of the National Academy of Sciences* 107.40 (2010): 17113-17118.
29. Butterfield, D. Allan, Aaron M. Swomley, and Rukhsana Sultana. "Amyloid β-peptide (1–42)-induced oxidative stress in Alzheimer disease: importance in disease pathogenesis and progression." *Antioxidants & redox signaling* 19.8 (2013): 823-835.
30. Ahmad, Waqar et al. "Oxidative toxicity in diabetes and Alzheimer's disease: mechanisms behind ROS/ RNS generation." *Journal of biomedical science* vol. 24,1 76. 19 Sep. 2017, doi:10.1186/s12929-017-0379-z
31. Lee, Hyoung-gon, et al. "Amyloid-Beta in Alzheimer Disease: The Null Versus the Alternate Hypotheses." *The Journal of Pharmacology and Experimental Therapeutics*, vol. 321, no. 3, 2007, pp. 823-829.
32. Smith, Danielle G., Roberto Cappai, and Kevin J. Barnham. "The redox chemistry of the Alzheimer's disease amyloid β peptide." *Biochimica et Biophysica Acta (BBA)-Biomembranes*1768.8 (2007): 1976-1990.
33. Kontush, A. "Amyloid-Beta: An Antioxidant that Becomes a Pro-Oxidant and Critically Contributes to Alzheimer's Disease." *Free Radical Biology & Medicine*, vol. 31, no. 9, 2001, pp. 1120.
34. Pedersen, Jeppe T., et al. "Amyloid-β and α-synuclein decrease the level of metal-catalyzed reactive oxygen species by radical scavenging and redox silencing." *Journal of the American Chemical Society* 138.12 (2016): 3966-3969.
35. Nadal, Rebecca C., Stephen EJ Rigby, and John H. Viles. "Amyloid β− Cu2+ complexes in both monomeric and fibrillar forms do not generate H2O2 catalytically but quench hydroxyl radicals." *Biochemistry* 47.44 (2008): 11653-11664.
36. Huang, Ling, Tao Su, and Xingshu Li. "Natural products as sources of new lead compounds for the treatment of Alzheimer's disease." *Current topic*
37. Ehrnhoefer, Dagmar E., et al. "EGCG redirects amyloidogenic polypeptides into unstructured, off-pathway oligomers." *Nature structural & molecular biology* 15.6 (2008): 558.
38. Schmidt, Matthias, et al. "Comparison of Alzheimer Aβ (1–40) and Aβ (1–42) amyloid fibrils reveals similar protofilament structures." *Proceedings of the National Academy of Sciences*106.47 (2009): 19813-19818.
39. Mehta, Akul. "Ultraviolet-visible (UV-Vis) spectroscopy-derivation of beer-lambert law." *Analytical Chemistry. Available at pharmaxchange. info* (2012).

40. Perkampus, Heinz-Helmut. *UV-VIS Spectroscopy and its Applications*. Springer Science & Business Media, 2013.
41. Lakowicz, Joseph R., ed. *Principles of fluorescence spectroscopy*. Springer Science & Business Media, 2013.
42. Mehta, Akul. "Animation for the Principle of Fluorescence and UV-Visible Absorbance." *Analytical Chemistry, Animations, Notes* (2013).
43. Eberhardt, Manfred K., and Ramon Colina. "The reaction of OH radicals with dimethyl sulfoxide. A comparative study of Fenton's reagent and the radiolysis of aqueous dimethyl sulfoxide solutions." *The Journal of Organic Chemistry* 53.5 (1988): 1071-1074.
44. Panche, A. N., A. D. Diwan, and S. R. Chandra. "Flavonoids: an overview." *Journal of nutritional science* 5 (2016).
45. Mira, Lurdes, et al. "Interactions of flavonoids with iron and copper ions: a mechanism for their antioxidant activity." *Free radical research* 36.11 (2002): 1199-1208.
46. Seo, Suho, et al. "Isorhamnetin Inhibits Reactive Oxygen Species-Dependent Hypoxia Inducible Factor (HIF)-1α Accumulation." *Biological and Pharmaceutical Bulletin*, vol. 39, no. 11, 2016, pp. 1830-1838.
47. Holland, Thomas M., et al. "Dietary Flavonols and Risk of Alzheimer Dementia." *Neurology*, 2020, pp. 10.
48. Céspedes, Carlos L., et al. "Antifungal and Antibacterial Activities of Mexican Tarragon (Tagetes Lucida)." *Journal of Agricultural and Food Chemistry*, vol. 54, no. 10, 2006, pp. 3521-3527.
49. Felgines, Catherine, et al. "Bioavailability of the Flavanone Naringenin and its Glycosides in Rats." *American Journal of Physiology - Gastrointestinal and Liver Physiology*, vol. 279, no. 6, 2000, pp. 1148-1154.
50. Yáñez, Jaime A., Preston K. Andrews, and Neal M. Davies. "Methods of Analysis and Separation of Chiral Flavonoids." *Journal of Chromatography B*, vol. 848, no. 2, 2007, pp. 159-181.
51. Choudhury, Ruksana, et al. "Interactions of the flavonoid naringenin in the gastrointestinal tract and the influence of glycosylation." *Biochemical and biophysical research communications* 265.2 (1999): 410-415.
52. Heo, Ho Jin, et al. "Effect of antioxidant flavanone, naringenin, from Citrus junos on neuroprotection." *Journal of Agricultural and Food Chemistry* 52.6 (2004): 1520-1525.
53. De Strooper, Bart, and Wim Annaert. "Proteolytic processing and cell biological functions of the amyloid precursor protein." *Journal of cell science* 113.11 (2000): 1857-1870.
54. Zheng, Hui, and Edward H. Koo. "The amyloid precursor protein: beyond amyloid." *Molecular neurodegeneration* 1.1 (2006): 5.
55. Chen, Fusheng, et al. "TMP21 is a presenilin complex component that modulates γ-secretase but not ε-secretase activity." *Nature* 440.7088 (2006): 1208-1212.